Near-Optimal Detection of Zak-OTFS Signals

Fathima Jesbin and A. Chockalingam
Department of ECE, Indian Institute of Science, Bangalore

***Abstract*—Orthogonal time frequency space (OTFS) modulation is emerging as a promising alternative to currently deployed multicarrier modulation schemes, particularly in high-Doppler wireless channels. The multicarrier (MC) version of OTFS (MC-OTFS) has dominated the OTFS research literature so far due to its compatibility with the prevailing MC modulation schemes. Recently, Zak transform based OTFS (Zak-OTFS) has gained prominence on account of its superior performance and low complexity. However, unlike in its MC counterpart, the transceiver signal processing aspects like equalization/detection and channel estimation in Zak-OTFS remain vastly unexplored. In this paper, we present an early investigation of low-complexity detection algorithms for Zak-OTFS that can scale efficiently for large frame sizes and achieve near-optimal performance. For this, we resort to efficient local search algorithms, namely, likelihood ascent search (LAS) and reactive tabu search (RTS) algorithms, that scale well for large dimensions. To assess the closeness of the performance of these algorithms to the optimum maximum likelihood (ML) performance, we obtain a lower bound on ML performance via RTS simulation using the transmit vector as the initial vector and defining a suitable neighborhood. Our simulation results indicate that while the performance of the popularly known minimum mean square error (MMSE) and message passing (MP) algorithms are far from the ML performance bound, LAS and RTS algorithms initialized with MMSE solution achieve close to ML performance bound within about 1 dB at a bit error rate of 10^{-5}.**

***Index Terms*—OTFS modulation, delay-Doppler domain, Zak-OTFS, MC-OTFS, MMSE detection, MP detection, likelihood ascent search, reactive tabu search, ML lower bound.**

I. Introduction

The emergence of high mobility and high carrier frequency use cases in wireless communication systems leads to high-Doppler scenarios, adding time-selectivity to frequency-selective channels. The popular orthogonal frequency division multiplexing (OFDM) fails in these doubly-selective channels, prompting the exploration of alternative waveforms that are robust to rapid time variations in the channel. Orthogonal time frequency space (OTFS) modulation proposed in [1] is a promising modulation scheme for achieving reliable communication in high-Doppler channels. In OTFS, information symbols are multiplexed in the delay-Doppler (DD) domain. Moreover, the doubly-selective wireless channel is parameterized in the DD domain which renders a sparse and largely time-invariant representation, and this contributes to complexity and performance advantages.

Central to OTFS modulation is the conversion of DD domain symbols to time domain (TD) at the transmitter and vice versa at the receiver. This is carried out differently by different variants of OTFS. One popularly studied variant is the multicarrier OTFS (MC-OTFS), where the DD domain to TD conversion is carried out in two steps, viz., DD domain to time-frequency (TF) domain via inverse symplectic finite Fourier transform (ISFFT) followed by TF domain to TD conversion using Heisenberg transform [1]-[3]. This two-step approach has been at the forefront of OTFS research owing to its compatibility with existing multicarrier modulation schemes like OFDM [4]. Lately, Zak-OTFS, which offers a one-step conversion from DD domain to TD using inverse time Zak transform [5], has garnered research attention as it is more robust to a larger range of delay and Doppler spreads of the channel compared to that with MC-OTFS [6]-[10].

A comprehensive treatment of Zak-OTFS and its attributes is presented in [6],[7]. These recent works emphasize the attributes of Zak-OTFS, such as non-fading and predictability of the input-output (I/O) relation, and notes that these attributes allow the DD channel to be efficiently acquired and equalized, resulting in better robustness. Zak-OTFS waveform is a quasi-periodic DD domain pulse, localized within the fundamental period, which when converted to TD using inverse time Zak transform is a pulse train modulated by a frequency tone (referred to as pulsone). Aliasing in the DD domain is avoided by an appropriate choice of pulsone periods (ensuring operation in the crystalline regime where the crystallization condition is satisfied) and pulse shaping filters (DD localized pulses). The crystallization condition is said to be satisfied when the DD periods of the pulsone are chosen to be large compared to the DD channel spreads.

In [7], MC-OTFS is interpreted as a multicarrier approximation to Zak-OTFS, and a detailed comparison of I/O relation and bit error performance between Zak-OTFS and MC-OTFS is carried out. The bit error performance comparison is made considering minimum mean square error (MMSE) detection. MMSE detection, though attractive for its cubic complexity in the OTFS frame size, is not optimal. Optimum detection, on the other hand, is exponentially complex in the frame size and hence prohibitive. While several detection algorithms for MC-OTFS have been investigated in the literature [11]-[16], algorithms for Zak-OTFS signal detection remain unexplored. Specifically, performance of detection algorithms for Zak-OTFS other than MMSE detection has not been reported. The new contributions in this paper can be summarized as follows.

- Our work in this paper presents an early investigation of low-complexity detection algorithms for Zak-OTFS that can scale efficiently for large frame sizes and achieve near-optimal performance. For this, we resort to efficient local search algorithms that scale well for large dimen-

This work was supported in part by the J. C. Bose National Fellowship, Department of Science and Technology, Government of India.

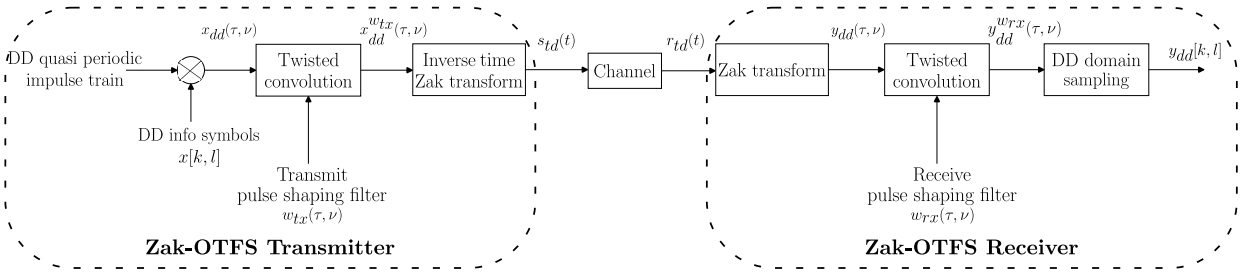

Fig. 1: Transceiver signal processing in Zak-OTFS.

sions [17]. These algorithms include likelihood ascent search (LAS) and reactive tabu search (RTS) algorithms.

- Our simulation results show that the LAS and RTS algorithms outperform the minimum mean square error (MMSE) and message passing (MP) algorithms popularly known in the OTFS literature.
- A key question we address in this paper is how close the considered search algorithms perform compared to the optimal detection performance. Towards this, we obtain a lower bound on ML performance via RTS simulation using the transmit vector as the initial vector and defining a suitable neighborhood and error counting. Simulation results indicate that while MMSE and MP detection performance are far from the ML performance bound, the LAS and RTS algorithms initialized with MMSE solution achieve close to ML performance bound within about 1 dB at a bit error rate (BER) of 10^{-5}.

The rest of the paper is organized as follows. Section II presents the Zak-OTFS system model. The considered algorithms for Zak-OTFS signal detection are presented in Sec. III. Performance results and discussions are presented in Sec. IV. Conclusions are presented in Sec. V.

II. Zak-OTFS system model

The block diagram in Fig. 1 illustrates the transceiver signal processing in Zak-OTFS. At the transmitter, the continuous DD domain signal, which is time- and bandwidth-limited, is converted into a TD signal for transmission via inverse-time-Zak transform. At the receiver, the received TD signal is converted back to the DD domain using Zak transform, followed by match-filtering and sampling for detection.

Zak-OTFS modulation is parameterized by τ_p and ν_p, which denote the delay and Doppler periods of the pulsone, respectively, related as $\tau_p\nu_p = 1$. The DD plane is partitioned into boxes/rectangles of length τ_p along the delay axis and ν_p along the Doppler axis, and the fundamental period in the DD domain is defined as

$$\mathcal{D}_0 \triangleq \{(\tau,\nu) : 0 \le \tau < \tau_p, 0 \le \nu < \nu_p\}, \tag{1}$$

where τ and ν represent the delay and Doppler variables, respectively. This is discretized to get the DD domain information grid as

$$\Lambda_{\rm dd} \triangleq \left\{ \left(k\frac{\tau_p}{M}, l\frac{\nu_p}{N}\right) \mid k = 0,\cdots,M-1, l = 0,\cdots,N-1 \right\}, \tag{2}$$

where the integers $M \approx B\tau_p$ and $N \approx T\nu_p$ are the number of delay and Doppler bins, respectively, and T, B denote the time duration and bandwidth of the pulsone, respectively [7].

The information symbols, $x[k,l], k = 0,\cdots,M-1$ and $l = 0,\cdots,N-1$, drawn from a modulation alphabet $\mathbb{A}$, are multiplexed on the DD information grid. The quasi-periodic discrete DD domain information signal, with delay period M and Doppler period N, is given by

$$x_{\rm dd}[k+nM, l+mN] = x[k,l]e^{j2\pi n\frac{l}{N}}, \quad m,n \in \mathbb{Z}. \tag{3}$$

The continuous DD domain information signal is given by

$$x_{\rm dd}(\tau,\nu) = \sum_{k,l\in\mathbb{Z}} x_{\rm dd}[k,l]\delta\left(\tau - k\frac{\tau_p}{M}\right)\delta\left(\nu - l\frac{\nu_p}{N}\right),$$

where $\delta(\cdot)$ denotes the Dirac-delta impulse function. Twisted convolution of the signal with DD domain transmit pulse $w_{\rm tx}(\tau,\nu)$ results in time- and bandwidth-limited DD domain transmit signal, given by [7]

$$x_{\rm dd}^{w_{\rm tx}}(\tau,\nu) = w_{\rm tx}(\tau,\nu) *_\sigma x_{\rm dd}(\tau,\nu),$$

where $*_\sigma$ denotes the twisted convolution operation[1]. The TD transmit signal is realized by applying the inverse-time-Zak transform[2], given by

$$s_{\rm td}(t) = \mathcal{Z}_t^{-1}\left(x_{\rm dd}^{w_{\rm tx}}(\tau,\nu)\right). \tag{4}$$

The DD domain channel representation is specified by the DD spreading function $h(\tau,\nu)$, given by

$$h(\tau,\nu) = \sum_{i=1}^{P} h_i\delta(\tau-\tau_i)\delta(\nu-\nu_i), \tag{5}$$

where P denotes the number of DD channel paths, and h_i, τ_i, and ν_i denote the complex channel gain, delay, and Doppler, respectively, associated with the ith path. The received TD signal at the receiver is then given by

$$r_{\rm td}(t) = \iint h(\tau,\nu)s_{\rm td}(t-\tau)e^{j2\pi\nu(t-\tau)}d\tau\, d\nu + n_{\rm td}(t), \tag{6}$$

where $n_{\rm td}(t)$ is the AWGN. The received TD signal is converted to DD domain signal $y_{\rm dd}(\tau,\nu)$ via Zak transform[3] as

$$y_{\rm dd}(\tau,\nu) = \mathcal{Z}_t\left(r_{\rm td}(t)\right). \tag{7}$$

[1] $x(\tau,\nu) *_\sigma y(\tau,\nu) \triangleq \iint x(\tau',\nu')y(\tau-\tau',\nu-\nu')e^{j2\pi\nu'(\tau-\tau')}d\tau'\, d\nu'$

[2] $\mathcal{Z}_t^{-1}\left(x(\tau,\nu)\right) \triangleq \sqrt{\tau_p}\int_0^{\nu_p} x(t,\nu)d\nu$

[3] $\mathcal{Z}_t\left(z(t)\right) \triangleq \sqrt{\tau_p}\sum_{k\in\mathbb{Z}} z(\tau+k\tau_p)e^{-j2\pi\nu k\tau_p}$

The action of the channel on the DD domain transmit signal is given by twisted convolution operation as

$$y_{\rm dd}(\tau,\nu) = h(\tau,\nu) *_\sigma x_{\rm dd}^{w_{\rm tx}}(\tau,\nu) + n_{\rm dd}(\tau,\nu), \quad (8)$$

where $n_{\rm dd}(\tau,\nu) = \mathcal{Z}_t\left(n_{\rm td}(t)\right)$. The DD signal in (8) is match-filtered with the DD domain receive pulse shaping filter $w_{\rm rx}(\tau,\nu)$, i.e., $y_{\rm dd}^{w_{\rm rx}}(\tau,\nu) = w_{\rm rx}(\tau,\nu) *_\sigma y_{\rm dd}(\tau,\nu)$, which can be derived as [7]

$$y_{\rm dd}^{w_{\rm rx}}(\tau,\nu) = h_{\rm dd}(\tau,\nu) *_\sigma x_{\rm dd}(\tau,\nu) + n_{\rm dd}^{w_{\rm rx}}(\tau,\nu), \quad (9)$$

where $n_{\rm dd}^{w_{\rm rx}}(\tau,\nu) = w_{\rm rx}(\tau,\nu) *_\sigma n_{\rm dd}(\tau,\nu)$ and $h_{\rm dd}(\tau,\nu)$ is the effective continuous DD channel filter, defined as

$$h_{\rm dd}(\tau,\nu) \triangleq w_{\rm rx}(\tau,\nu) *_\sigma h(\tau,\nu) *_\sigma w_{\rm tx}(\tau,\nu). \quad (10)$$

The match-filtered received signal is then sampled on the DD domain information grid to get the discrete DD domain received signal

$$y_{\rm dd}[k,l] = y_{\rm dd}^{w_{\rm rx}}\Big(\tau = k\frac{\tau_p}{M}, \nu = l\frac{\nu_p}{N}\Big), \quad k,l \in \mathbb{Z}. \quad (11)$$

The input-output relation is given by a discrete twisted convolution operation as

$$y_{\rm dd}[k,l] = h_{\rm dd}[k,l] *_\sigma x_{\rm dd}[k,l] + n_{\rm dd}[k,l], \quad (12)$$

where $n_{\rm dd}[k,l]$ is the noise sample and $h_{\rm dd}[k,l]$ denotes the effective discrete DD channel filter output which is obtained by sampling the effective continuous DD channel filter output, i.e.,

$$h_{\rm dd}[k,l] = h_{\rm dd}\Big(\tau = k\frac{\tau_p}{M}, \nu = l\frac{\nu_p}{N}\Big), \quad k,l \in \mathbb{Z}. \quad (13)$$

Substituting the definition of twisted convolution in (12), we have the complete input-output relation as

$$y_{\rm dd}[k,l] = \sum_{k',l' \in \mathbb{Z}} h_{\rm dd}[k-k', l-l'] x_{\rm dd}[k',l'] e^{j2\pi \frac{(l-l')k'}{MN}} + n_{\rm dd}[k,l]. \quad (14)$$

A. Vectorized formulation of input-output relation

Owing to the quasi-periodicity in the DD domain, it is sufficient to consider the received samples within the fundamental period. Then, the expression in (14) for the MN samples can be vectorized to get

$$\mathbf{y} = \mathbf{H}\mathbf{x} + \mathbf{n}, \quad (15)$$

where $\mathbf{x}, \mathbf{y}, \mathbf{n} \in \mathbb{C}^{MN\times 1}$, such that their $(kN+l+1)$th entries are given by $x_{kN+l+1} = x_{\rm dd}[k,l]$, $y_{kN+l+1} = y_{\rm dd}[k,l]$, $n_{kN+l+1} = n_{\rm dd}[k,l]$, and $\mathbf{H} \in \mathbb{C}^{MN\times MN}$ such that

$$\mathbf{H}[k'N+l'+1, kN+l+1] = \sum_{m,n\in\mathbb{Z}} h_{\rm dd}[k'-k-nM, l'-l-mN] \; e^{j2\pi nl/N} e^{j2\pi \frac{(l'-l-mN)(k+nM)}{MN}}, \quad (16)$$

where $k', k = 0, \cdots, M-1, l', l = 0, \cdots, N-1$, and the entries of $\mathbf{n}$ are distributed as $\mathcal{CN}(0,\sigma^2)$.

III. Algorithms for Zak-OTFS signal detection

Zak-OTFS signal detection algorithms investigated in this paper are described in the following subsections.

A. LMMSE detection

Linear detectors perform data detection using a linear transformation matrix (say, $\mathbf{G}$) and a mapping function (say, f) as

$$\hat{\mathbf{x}} = f(\mathbf{G}\mathbf{y}). \quad (17)$$

The function $f(.)$ maps each entry of the transformed received vector $\mathbf{G}\mathbf{y}$ to a symbol in the modulation alphabet $\mathbb{A}$ based on minimum Euclidean distance. For the I/O relation in (15), the transformation matrix for LMMSE detection is

$$\mathbf{G} = (\mathbf{H}^H\mathbf{H} + \sigma^2\mathbf{I})^{-1}\mathbf{H}^H. \quad (18)$$

Since the computation of $\mathbf{G}$ necessitates the inversion of $MN \times MN$ matrices, it leads to a computational complexity of $\mathcal{O}(M^3N^3)$, which is for a total of MN symbols. Hence, the complexity per symbol is $\mathcal{O}(M^2N^2)$. The BER results of Zak-OTFS reported in [6],[7] use this detection.

B. Message passing (MP) detection

The message passing (MP) algorithm used for MC-OTFS signal detection in [11] is an approximate maximum a posteriori (MAP) detector based on low-complexity message passing on graphical models. It uses a bipartite graph with variable nodes (x) and observation nodes (y) and iteratively passes messages between them. It involves the computation of approximate a posteriori probabilities of the modulation symbols by passing messages on the graph. This algorithm was inspired by the large MIMO detection algorithm in [18], which approximates the interference from multiple antennas as Gaussian, and this reduced the complexity of the computation of messages. While the graph in [18] is a fully connected graph (because the MIMO channel matrix is such that every observation node is influenced by all the variable nodes), the graph in [11] is sparsely connected (because of the sparse nature of the effective channel matrix in MC-OTFS). MC-OTFS detection leverages this intrinsic sparsity to further reduce the message computation complexity. On the other hand, the effective channel matrix in Zak-OTFS, i.e., matrix $\mathbf{H}$ in (15), is not sparse, resulting in a fully connected graph. Still, the Gaussian approximation of interference in the algorithm results in cubic complexity in the frame size, which (like MMSE detection) is affordable. To enhance the convergence of the iterative algorithm, we employ damping where messages are computed as a convex combination of the current and previous messages, with the damping factor serving as the weight for the current message.

C. LAS algorithm

Likelihood ascent search (LAS) detector is a low-complexity local search based detector [17]. The algorithm starts with an initial solution vector and searches for better solution vectors (in terms of ML cost $\|\mathbf{y} - \mathbf{H}\mathbf{x}\|^2$) in the neighborhood till a local minima is reached. It starts by declaring the initial solution vector as the current solution vector and checks if the best among the neighbors of the current solution vector is better (in terms of ML cost) than the current solution vector. If yes, the best neighbor is declared

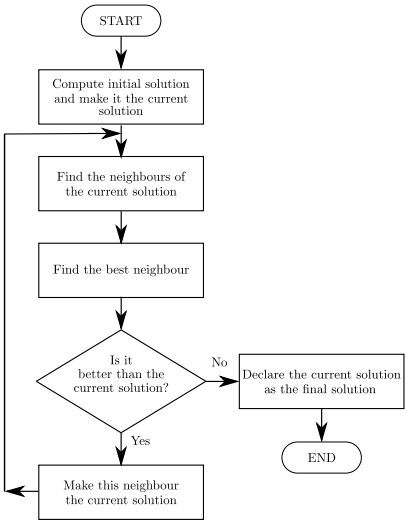

Fig. 2: Flowchart of the LAS algorithm.

as the current solution vector and the algorithm proceeds to the next iteration. In the next iteration, the neighborhood of the new current solution vector is tested for a better solution vector. This process continues till the current solution vector is the best in its neighborhood, i.e., the algorithm has reached a local minima, and the algorithm stops. The current solution vector in the last iteration is declared as the detected vector. The flow chart of the LAS algorithm is shown in Fig. 2.

Neighborhood definition: The search complexity of the algorithm depends on the definition and size of the neighborhood. For example, consider a *1-symbol away neighborhood*, where the neighborhood consists of all the vectors which differ from the current solution vector in only one coordinate. The size of this neighborhood grows only linearly in the frame size, and this reduces the search complexity. A k-symbol away neighborhood, $k > 1$, where the neighbors differ from the current solution vector in up to k coordinates has a larger neighborhood size. The quality of the detected vector can be better because of the larger search space, but at the cost of increased search complexity. In problems with large dimensions, LAS algorithm with a simple 1-symbol away neighborhood gives good solution vectors. Also, the quality of the solution depends on the initial solution with which the algorithm starts. A better initial vector leads to a better solution vector. For the Zak-OTFS detection in this paper, we use the 1-symbol away neighborhood definition and use MMSE solution vector as the initial solution vector. Consequently, the algorithm is called the MMSE-LAS algorithm.

Complexity: The initial solution computation and the search operation contribute to the computational complexity of LAS. Since the search part is random, the average complexity of the search operation is obtained through simulations, which is $\mathcal{O}(MN)$ per symbol [17]. The complexity of the MMSE solution is $\mathcal{O}(M^2N^2)$ per symbol, as a total of MN symbols are involved. Clearly, for large dimensions, the overall complexity is dominated by the initial solution computation.

D. RTS algorithm

The RTS algorithm [17] also uses an iterative local neighborhood search based approach, but, unlike LAS, it has a wider search space as it employs an escape strategy from the local minima. This feature prevents the algorithm from being trapped in the first encountered local minima, enabling exploration beyond the neighborhood of the initial solution vector. RTS traces through different neighborhoods until it satisfies the specified stopping criterion. To enhance search efficiency, revisits to the solutions are allowed only in a controlled manner by using a tabu period. Tabu period is the number of iterations for which the revisit to a particular solution is prohibited (hence the name 'tabu'), which is dynamically changed based on the frequency of revisits (fixed tabu search is a variant that keeps the tabu period constant). The tabu solutions are tracked using a tabu matrix. The complexity analysis in [17] through simulations illustrates a higher complexity for RTS search operation than its LAS counterpart, which is intuitive since the former has a broader search space. This makes RTS to achieve better performance compared to LAS at the cost of some complexity increase. However, the overall complexity, primarily dominated by the computation of the initial solution, does not exhibit a significant difference for higher dimensions. In the RTS also, we employ 1-symbol away neighborhood and use MMSE solution vector as the initial vector. Consequently, the algorithm is called MMSE-RTS algorithm.

1) Lower bound on ML performance: In the next section on results and discussions, we will present the simulated BER performance of the detectors presented above. It is of interest, however, to know how far are these detectors from the optimum ML detector in terms of bit error performance. Simulation of ML performance for frame sizes considered in the results and discussions section is prohibitive. Hence, we compute a lower bound on the ML performance via RTS simulations as outlined in [19], which is complexity-wise feasible. To obtain the ML lower bound through RTS simulation, the RTS algorithm starts with the transmitted vector as the initial solution. The n-symbol neighborhood of a vector is defined as the set of all vectors differing from it in i coordinates, $1 \leq i \leq n$. Depending on the location of the final solution vector relative to the bound specified by the n-symbol neighborhood definition, a lower bound for the number of symbol errors in the ML solution vector, e_{ML}, is computed as

$$e_{ML} = \begin{cases} e_{RTS}, & \text{if } e_{RTS} \leq n \\ n+1, & \text{otherwise,} \end{cases}$$

where e_{RTS} denotes the number of symbol errors in the final solution vector compared to the initial vector (which is taken to be the transmit vector). The tightness of the bound can be improved using larger values of n, i.e., a larger neighborhood size, at the cost of higher complexity.

An approximate ML performance: Motivated by the high complexity needed to obtain a tighter bound (using larger n values), a low complexity approximation to the true ML

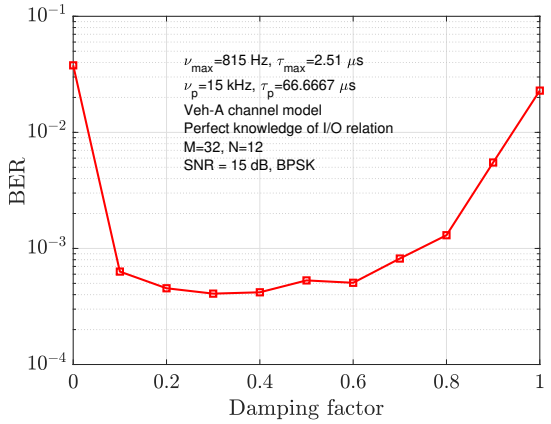

Fig. 3: BER performance of MP detection of Zak-OTFS as a function of damping factor.

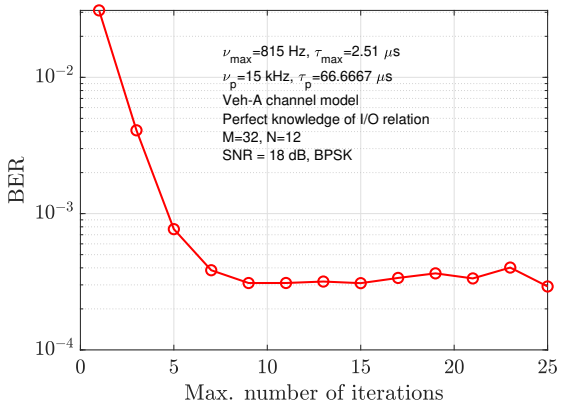

Fig. 4: Convergence behaviour of MP detection of Zak-OTFS.

performance can be obtained using the RTS algorithm [19]. This is obtained by running the RTS algorithm using the transmitted vector as the initial vector. The idea is that the e_{RTS} is an upper bound to the lower bound of ML symbol error count (e_{ML}). But it need not be a bound for the true ML performance. Hence, it is only an approximation. However, it is shown to be closer to the true ML at low SNR values.

IV. Results and Discussions

In this section, we illustrate the BER performance of the aforementioned detectors and demonstrate their performance proximity to ML detection performance. In all the simulations, we consider a Zak-OTFS system whose frame duration is fixed at $T = 0.8$ ms and bandwidth at $B = 480$ kHz. The Doppler period of the pulsone is set at $\nu_p = 15$ kHz, resulting in a corresponding delay period $\tau_p = 1/\nu_p = 66.6$ μs. Consequently, the system is characterized by $M = B\tau_p = 32$ delay bins and $N = T\nu_p = 12$ Doppler bins.

We consider the Vehicular-A channel model having six paths with a maximum Doppler shift $\nu_{\max} = 815$ Hz and power delay profile as given in [7]. We assume perfect knowledge of the I/O relation. Here, it can be easily verified that we are operating in deep crystalline regime (the delay period $\tau_p = 66.6$ μs is far greater than the channel delay spread $\tau_{max} = 2.51$ μs and the Doppler period $\nu_p = 15$ kHz significantly exceeds the channel Doppler spread of 1.63 kHz). The Doppler shift of the ith path is generated using Jakes' formula, $\nu_i = \nu_{\max}\cos\theta_i$, where θ_i values are independent and uniformly distributed in the interval $[0, 2\pi)$. Data symbols are drawn from BPSK modulation alphabet. The transmit and receive pulse shaping filters used are sinc filters, given by

$$w_{\text{tx}}(\tau,\nu) = w_{\text{rx}}(\tau,\nu) = \sqrt{BT}sinc(B\tau)sinc(T\nu).$$

In order to identify the optimal value of damping factor in the MP algorithm, we examine the BER performance as a function of the damping factor at an SNR value fixed at 15 dB. A maximum of 20 iterations of message passing is used. The results are shown in Fig. 3. It is observed that the algorithm performs poorly at the extreme values of the damping factor. When the damping factor equals 1, it corresponds to no damping, wherein all weight is assigned to the current message while disregarding the preceding one. At the opposite extreme corresponding to a damping value of 0, the current solution is entirely dismissed which also leads to inferior performance. From the plot, we obtain the optimal value to be 0.3, which is adopted for subsequent simulations. In Fig. 4, the convergence behaviour of the MP detection algorithm is studied by plotting the BER performance as a function of the maximum number of iterations, at 18 dB SNR. It can be observed that convergence occurs in as few as 10 iterations.

Figure 5 compares the BER performance of the various detectors, alongside the ML performance lower bounds obtained for $n = 1$ and 2. Although $n = 1$ gives the bound with a lower complexity, $n = 2$ gives a tighter bound at the cost of complexity, making it a better reference to compare the near-optimal performance of the various detectors. It can be seen that the MMSE detection yields subpar BER performance. MP detection outperforms MMSE detection at low to medium SNRs (by about 1.5 dB at 10^{-3} BER). But the MP detection performance is found to floor at high SNRs (beyond 15 dB), even performing poorer than MMSE detection. Regardless, both MP and MMSE performances are far from the ML performance bound. However, it can be observed that the MMSE-LAS and MMSE-RTS algorithms achieve close to ML performance bound ($n = 2$) within about 1 dB at 10^{-5} BER, in the high SNR regime. It is noteworthy that this performance improvement comes with a little additional search complexity compared to the MMSE complexity. In Fig. 6, it is seen that while the BER performance of MMSE-LAS and MMSE-RTS detectors are close to the ML lower bound at high SNRs, they are also close to the approximate ML performance at lower SNRs, highlighting their closeness to ML performance even at lower SNR values.

V. Conclusions

Our work in this paper demonstrated near-optimal performance of Zak-OTFS signal detection at low complexities that scale well for large frame sizes. Our results showed that the MMSE and MP detectors, though popular in the MC-OTFS

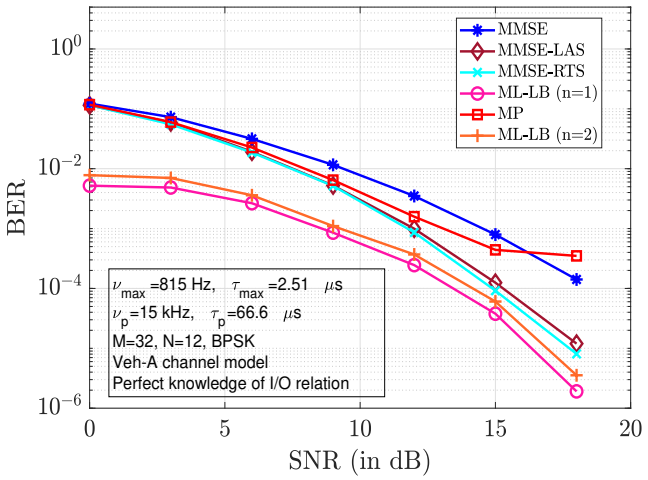

Fig. 5: BER performance of MMSE, MP, MMSE-LAS, MMSE-RTS detection of Zak-OTFS and ML performance lower bound for $n = 1, 2$.

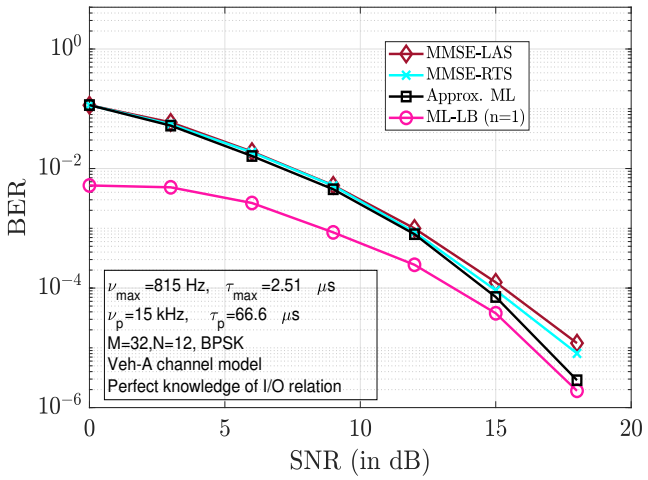

Fig. 6: BER performance of MMSE-LAS, MMSE-RTS detection of Zak-OTFS, ML performance lower bound, and approximate ML performance for $n = 1$.

literature, perform far from the optimum ML performance. On the other hand, simple local search based detectors such as LAS and RTS detectors were found to achieve near-ML performance with some additional search complexity. We demonstrated this by obtaining a lower bound for the ML performance via RTS simulation with a suitable choice of initial vector, neighborhood definition, and symbol error counting. We note that DD domain signal processing for Zak-OTFS is wide open for research, and the results reported in this work could trigger a broader research interest in DD signal processing for Zak-OTFS in general, and devising efficient detection and channel estimation algorithms for Zak-OTFS in particular.

REFERENCES

[1] R. Hadani *et al.*, "Orthogonal time frequency space modulation," *Proc. IEEE WCNC'2017*, pp. 1-6, Mar. 2017.

[2] S. S. Das, R. Prasad, *OTFS: Orthogonal Time Frequency Space Modulation - A Waveform for 6G*, River Publishers, 2022.

[3] Y. Hong, T. Thaj, and E. Viterbo, *Delay-Doppler Communications: Principles and Applications*, Academic Press, 2022.

[4] "Best Readings in Orthogonal Time Frequency Space (OTFS) and Delay Doppler Signal Processing," June 2022. https://www.comsoc.org/publications/best-readings/orthogonal-time-frequency-space-otfs-and-delay-doppler-signal-processing

[5] A. J. E. M. Janssen, "The Zak transform: A signal transform for sampled time-continuous signals", Philips J. Res., vol. 43, pp. 23-69, 1988.

[6] S. K. Mohammed, R. Hadani, A. Chockalingam, and R. Calderbank, "OTFS - a mathematical foundation for communication and radar sensing in the delay-Doppler domain," *IEEE BITS the Information Theory Magazine*, vol. 2, no. 2, pp. 36-55, 1 Nov. 2022.

[7] S. K. Mohammed, R. Hadani, A. Chockalingam, and R. Calderbank, "OTFS - predictability in the delay- Doppler domain and its value to communication and radar sensing," *IEEE BITS the Information Theory Magazine*, IEEE early access, doi: 10.1109/MBITS.2023.3319595.

[8] S. K. Mohammed, "Derivation of OTFS modulation from first principles," *IEEE Trans. Veh. Tech.*, vol. 70, no. 8, pp. 7619-7636, Aug. 2021.

[9] F. Lampel, A. Avarado, and F. M. J. Willems, "On OTFS using the discrete Zak transform," *Proc. IEEE ICC'2022 Workshops*, pp. 729-734, May 2022.

[10] V. Yogesh, V. S. Bhat, S. R. Mattu, and A. Chockalingam, "On the bit error performance of OTFS modulation using discrete Zak transform," *Proc. IEEE ICC'2023*, pp. 741-746, May 2023.

[11] P. Raviteja, K. T. Phan, Y. Hong and E. Viterbo, "Interference cancellation and iterative detection for orthogonal time frequency space modulation," *IEEE Trans. Wireless Commun.*, vol. 17, no. 10, pp. 6501-6515, Aug. 2018.

[12] W. Yuan, Z. Wei, J. Yuan, and D. W. K. Ng, "A simple variational Bayes detector for orthogonal time frequency space (OTFS) modulation," *IEEE Trans. Veh. Tech.*, vol. 69, no. 7, pp. 7976-7980, Jul. 2020.

[13] H. Zhang and T. Zhang, "A low-complexity message passing detector for OTFS modulation with probability clipping," *IEEE Wireless Commun. Lett.*, vol. 10, No. 6, pp. 1271-1275, Jun. 2021.

[14] S. Li *et al.*, "Hybrid MAP and PIC detection for OTFS modulation," *IEEE Trans. Veh. Tech.*, vol. 70, no. 7, pp. 7193-7198, Jul. 2021.

[15] L. Xiang, Y. Liu, L-L. Yang, and L. Hanzo, "Gaussian approximate message passing detection of orthogonal time frequency space modulation," *IEEE Trans. Veh. Tech.*, vol. 70, no. 10, pp. 10999-11004, Oct. 2021.

[16] S. Li, W. Yuan, Z. Wei, and J. Yuan, "Cross domain iterative detection for orthogonal time frequency space modulation," *IEEE Trans. Wireless Commun.*, vol. 21, no. 4, pp. 2227-2242, Apr. 2022.

[17] A. Chockalingam and B. Sundar Rajan, *Large MIMO Systems*, Cambridge University Press, 2014.

[18] P. Som, T. Datta, N. Srinidhi, A. Chockalingam, and B. S. Rajan, "Low-complexity detection in large-dimension MIMO-ISI channels using graphical models," *IEEE J. Sel. Topics Sig. Proc.*, vol. 5, no. 8, pp. 1497-1511, Dec. 2011.

[19] N. Srinidhi, T. Datta, A. Chockalingam, and B. S. Rajan, "Layered tabu search algorithm for large-MIMO detection and a lower bound on ML performance," *IEEE Trans. Commun.*, vol. 59, no. 11, pp. 2955-2963, Nov. 2011.